

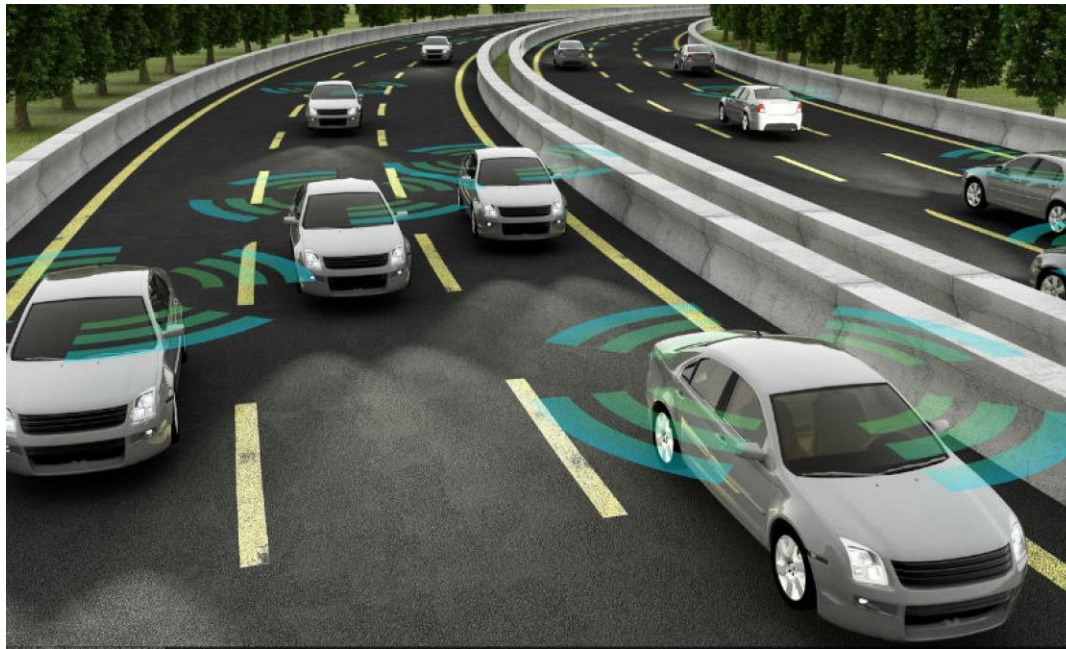
Adversarial Sensor Attack on LIDAR-based Perception

In Autonomous Driving

(Charles) Chengzeng You
Connected and autonomous vehicles
Department of computing
Email: cy19@ic.ac.uk

1. Introduction

Autonomous vehicles rely on perception, which leverages sensors like cameras and LiDARs (Light Detection and Ranging) to understand the surrounding driving environment.



1. Introduction

1.1 Sensor-level attacks

- camera blinding [42], physical-world camera attacks [28, 29], trojan attacks on the neural networks for AV camera input [37].
- A few works demonstrated the feasibility of injecting spoofed points into the sensor input from the LiDAR[42, 44].

The first study to explore the security of LiDAR-based perception in AV settings

1. Introduction

1.2 Existing spoofing techniques

- Machine learning output can be maliciously altered by carefully-crafted perturbations to the input [18, 20, 29, 41, 57].
- Formulating the attack task as an optimization problem has been proven effective in previous machine learning security studies [21, 24, 26, 50, 51, 53].

Strategically controlling the spoofed points to fool the machine learning model

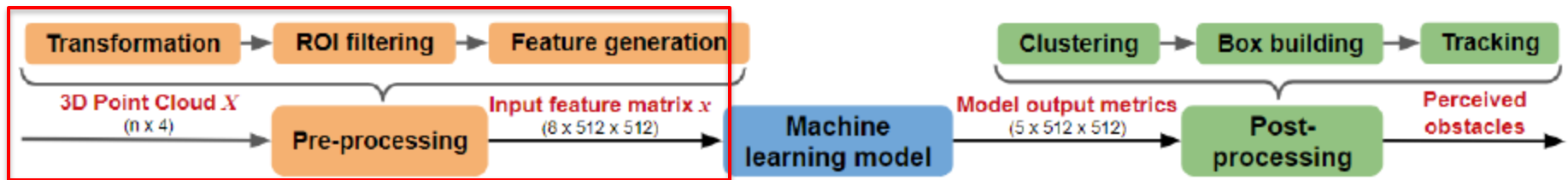
1. Introduction

1.3 Contributions

- The first security study of LiDAR-based perception for AV systems.
- Two methodology-level contributions: conduct experiments to analyze the LiDAR spoofing attack capability and design a global spatial transformation-based method to model such capability in mathematical forms; design an algorithm that combines optimization and global sampling.
- Case study: construct two potential attack scenarios: emergency brake attack and AV freezing attack.

2. Background

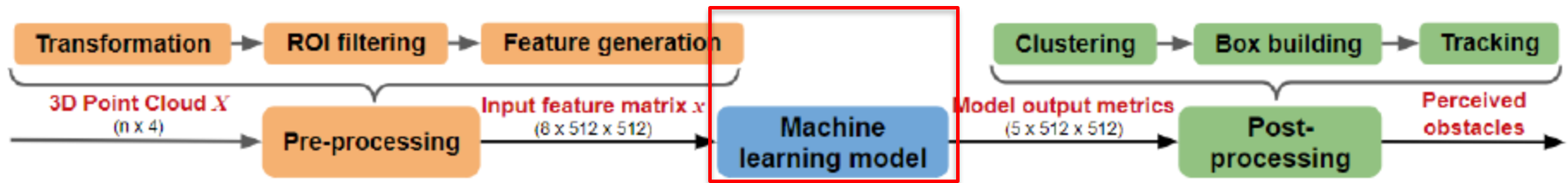
2.1 LiDAR-based Perception in AV Systems - Apollo



Input	Feature	Description
Trans	Max height	Maximum height of points in the cell.
ROI f	Max intensity	Intensity of the highest point in the cell.
outsid	Mean height	Mean height of points in the cell.
Featu	Mean intensity	Mean intensity of points in the cell.
cell 8	Count	Number of points in the cell.
	Direction	Angle of the cell's center with respect to the origin.
	Distance	Distance between the cell's center and the origin.
	Non-empty	Binary value indicating whether the cell is empty or occupied.

2. Background

2.1 LiDAR-based Perception in AV Systems - Apollo

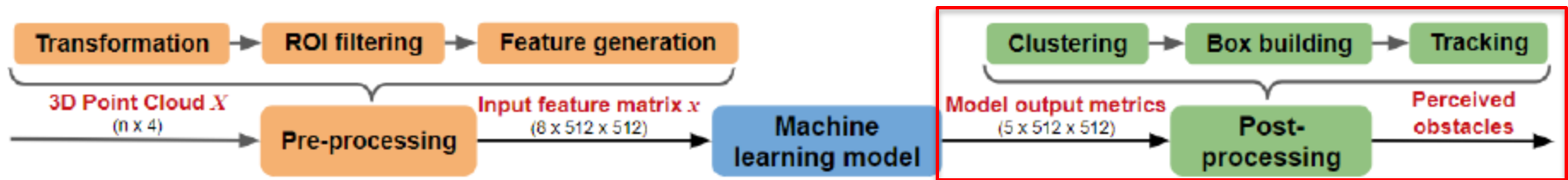


Deep
cell.
Output

Metrics	Description
Center offset	Offset to the predicted center of the cluster the cell belongs to.
Objectness	The probability of a cell belonging to an obstacle.
Positiveness	The confidence score of the detection.
Object height	The predicted object height.
Class probability	The probability of the cell being a part of a vehicle, pedestrian, etc.

2. Background

2.1 LiDAR-based Perception in AV Systems - Apollo



Input : cells with **objectness** greater than 0.5(by default)

Clustering : build candidate object clusters (connected graph) → select clusters greater than 0.1(by default)

Box building: reconstructs the bounding box including height, width, length of an obstacle candidate

Tracking: generate tracked obstacles

prediction module: predict the future trajectories of perceived obstacles

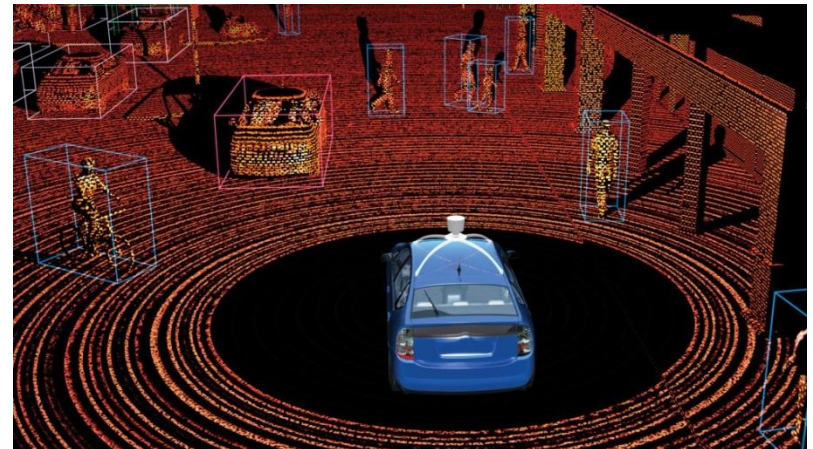
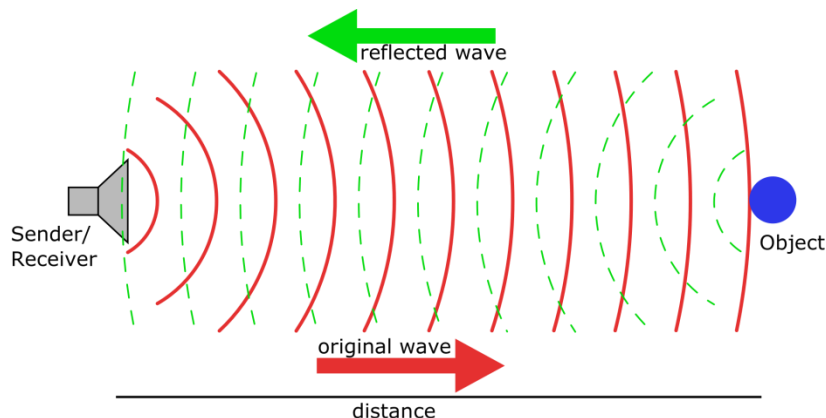
Planning module: plan the future driving routes and makes decisions

2. Background

2.2 LiDAR Sensor and Spoofing Attacks

Light Detection and Ranging (LiDAR) use laser to measure distance:

1. emitting a laser pulse on a surface
2. catching the reflected laser back to the LiDAR pulse source
3. measuring the time laser travelled
4. Distance = (Speed of light x Time elapsed) / 2



2. Background

2.2 LiDAR Sensor and Spoofing Attacks

Sensor spoofing attacks use the same physical channels as the targeted sensor to manipulate the sensor readings.

- place an attacking device at the roadside to shoot malicious laser pulses to AVs passing by.
- drive an attack vehicle equipped with an attacking device that shoots laser pulses to the victim AV's LiDAR.

LiDAR has been shown to be vulnerable to laser spoofing attacks

2. Background

2.3 Adversarial Machine Learning

Given a machine learning model M , input x and its corresponding label y , an **adversarial attacker** aims to generate adversarial examples x'

So that,

$$M(x') \neq y (\text{untargeted attack})$$

Or,

$$M(x') = y', \text{ where } y' \text{ is a target label (targeted attack).}$$

2. Background

2.3 Adversarial Machine Learning

Carlini and Wagner [21] proposed to generate an adversarial perturbation for a targeted attack:

$$\min ||\mathbf{x} - \mathbf{x}'||_p \quad \text{s.t. } M(\mathbf{x}') = \mathbf{y}' \text{ and } \mathbf{x}' \in X$$

More adversarial examples on:

segmentation [26, 53], human pose estimation [26], object detection [53], Visual Question Answer system [54], image caption translation [24], etc.

This paper also leverages an optimization-based method

3. Attack Goal and Threat Model

3.1 Attack goal

Fool the LiDAR-based perception into perceiving fake obstacles in front of a victim AV.

Target: front-near fake obstacles around 5 meters

3. Attack Goal and Threat Model

3.2 Threat model

Consider **LiDAR spoofing attacks** as the threat model, which is a demonstrated practical attack vector for LiDAR sensors.

Attacker has **white-box access** to the machine learning model and the perception system

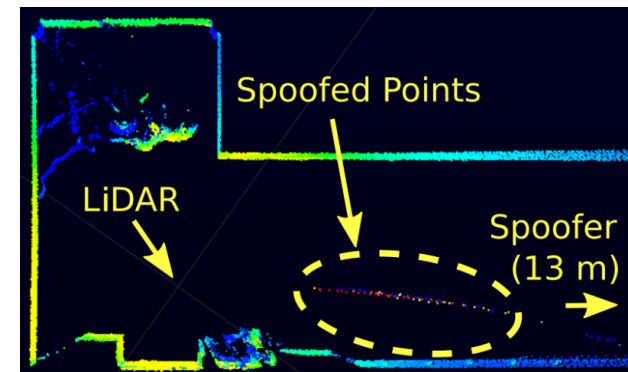
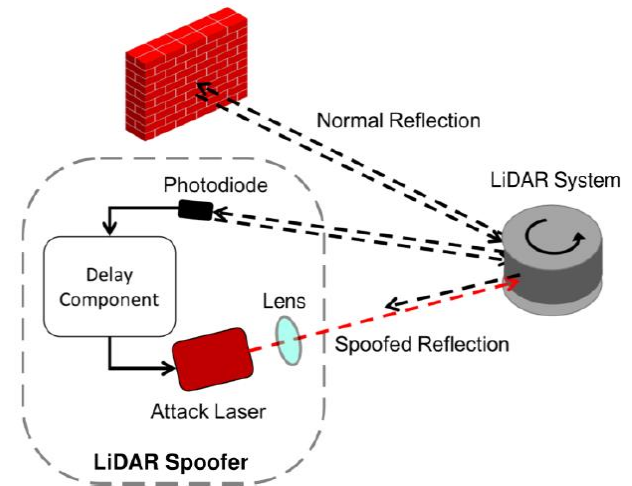
4. Methodology

4.1 Reproduce the LiDAR spoofing attack

Photodiode : trigger the delay component whenever it captures laser pulses fired from the victim LiDAR.

Delay component: trigger the attack laser after a certain amount of time

Results: In total, around **100 dots** can be spoofed.
Among **60 points at the center** 8-10 vertical lines can be stably spoofed with high intensity.



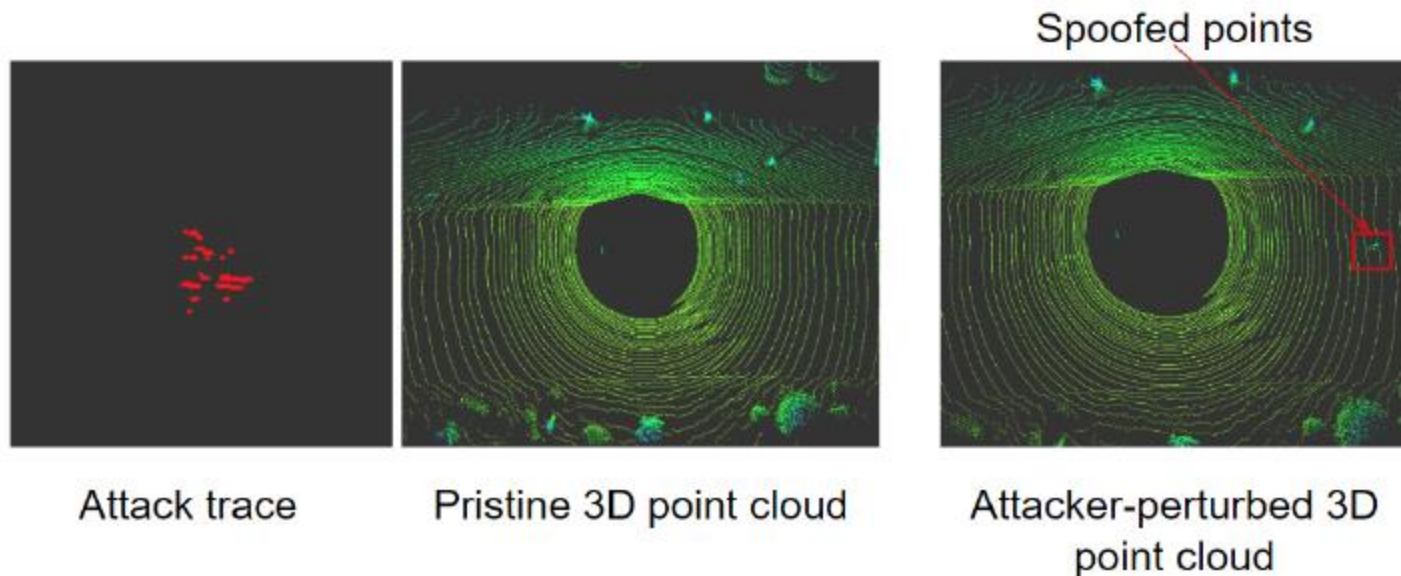
4. Methodology

4.2 Blind sensor spoofing

Experiment 1: Directly apply original spoofing attack traces.

Experiment 2: Apply spoofing attack traces at different angles.

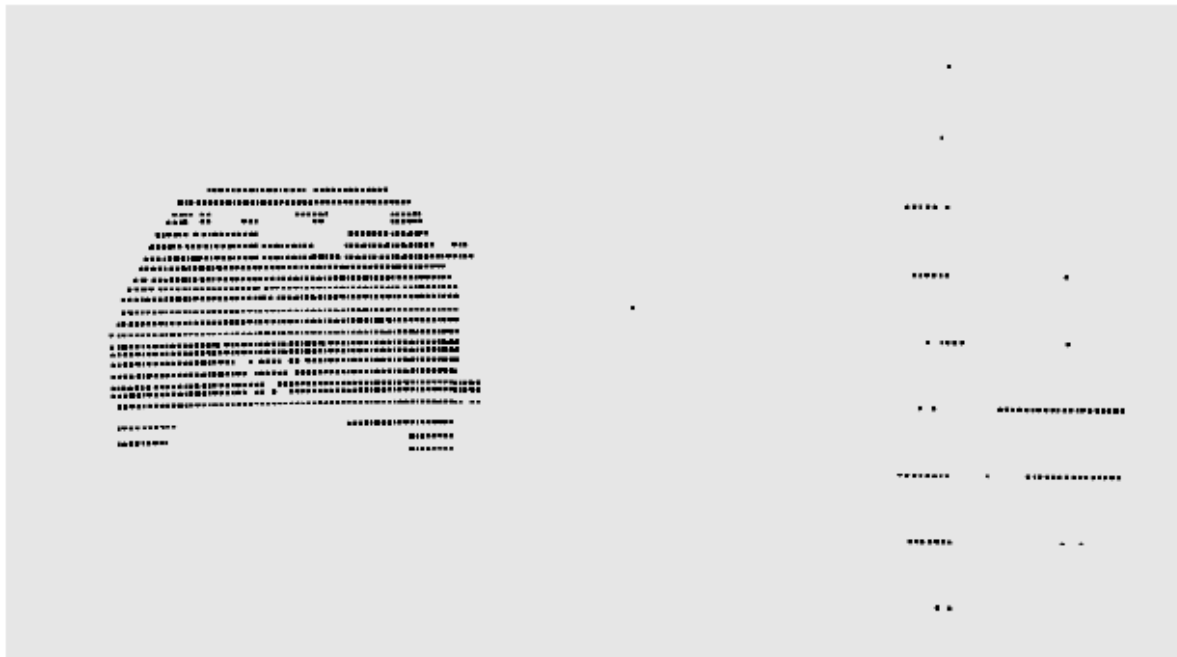
Experiment 3: Apply spoofing attack traces with different shapes



Failed to generate spoofed obstacles in the LiDAR-based perception pipeline in Baidu Apollo.

4. Methodology

4.2 Blind sensor spoofing



The point cloud for a real vehicle has a much wider angle and many more points than the attack traces.

4. Methodology

4.3 Adv-LiDAR overview

the problem is formulated as follows :

$$\begin{aligned} \min \quad & \mathcal{L}_{\text{adv}}(x \oplus t'; M) \\ \text{s.t.} \quad & t' \in \{\Phi(T') | T' \in \mathcal{A}\} \quad \& \quad x = \Phi(X) \end{aligned}$$

x : the corresponding 2D input feature matrix

t' : adversarial spoofed input feature matrix

$\oplus(\cdot)$: merging function

$\mathcal{L}_{\text{adv}}(\cdot; M)$: the adversarial loss, given the machine learning model

X : the pristine 3D point cloud

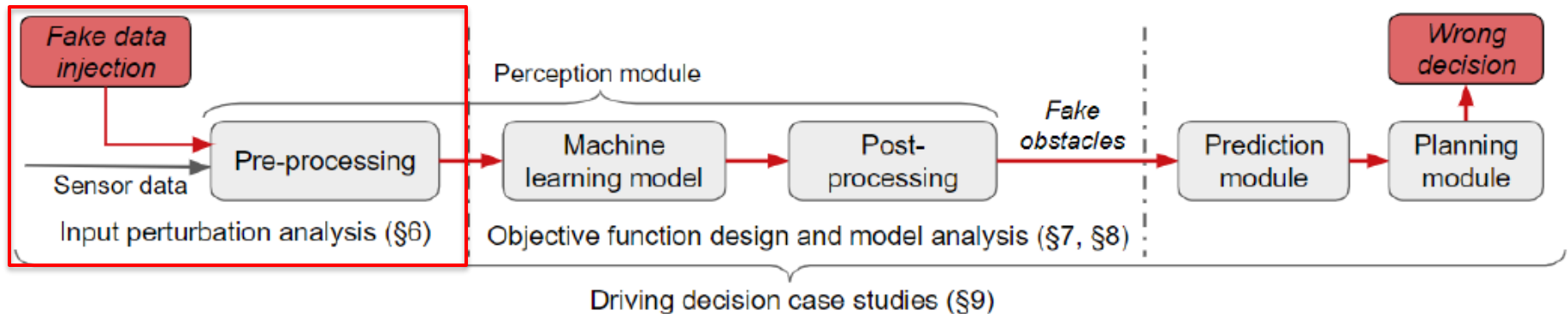
T' : adversarial spoofed 3D point cloud

\mathcal{A} : 3D point cloud generated from LiDAR spoofing attacks

$\Phi(\cdot)$: the pre-processing function that maps X into x

4. Methodology

4.3 Adv-LiDAR overview

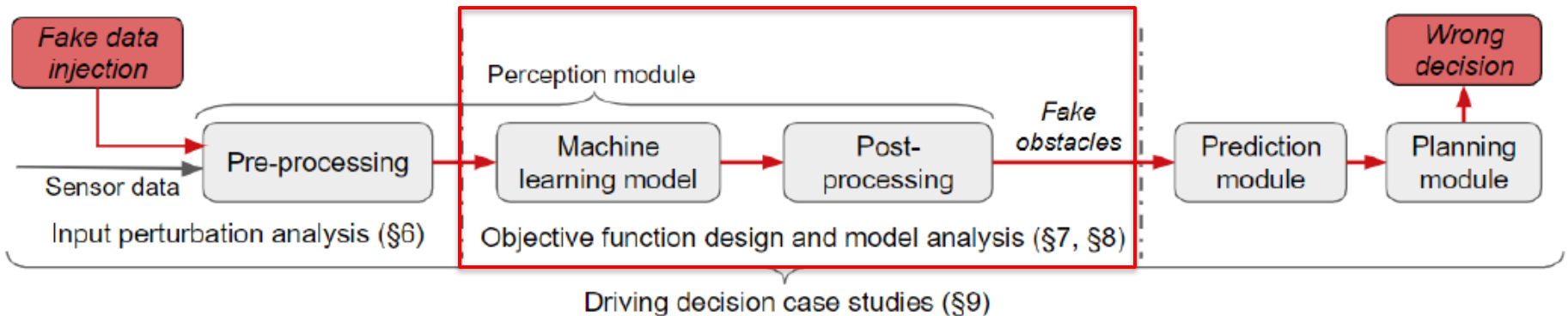


Input perturbation analysis:

1. conduct spoofing attacks on LiDAR to collect a set of possible spoofed 3D point cloud
2. model the spoofing attack capability **A**
3. formulate the spoofed input feature matrix into a differentiable function

4. Methodology

4.3 Adv-LiDAR overview

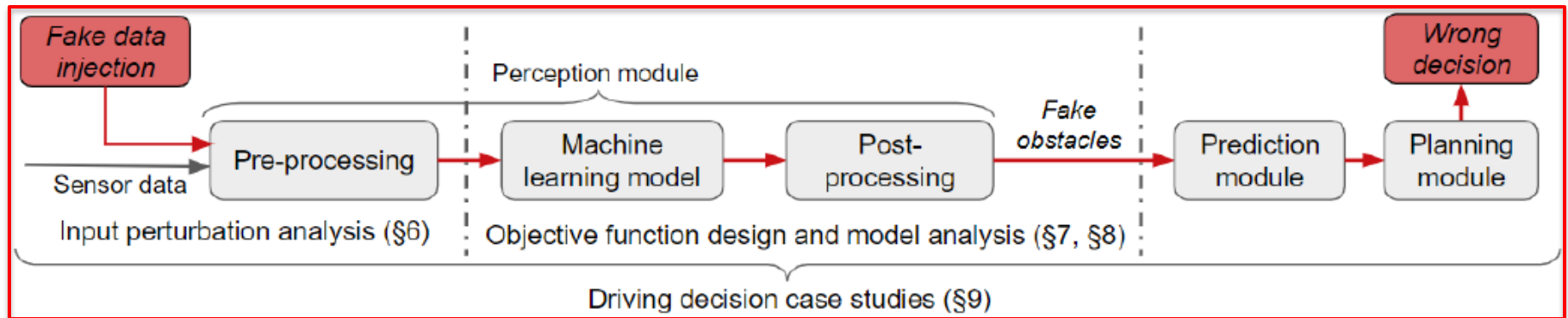


Objective function design and model analysis:

1. study the post-processing steps to extract key strategies of transforming model output into perceived obstacles, and formulate it into an **objective function**.
2. Instead of directly using existing optimization-based methods, we improve the methodology by **combining global sampling with optimization**.

4. Methodology

4.3 Adv-LiDAR overview



Driving decision case study:

1. generate adversarial 3D point cloud that can inject spoofed obstacles at the LiDAR-based perception level
2. model the spoofing attack capability
3. formulate the spoofed input feature matrix into a differentiable function

5. Input perturbation analysis

5.1 Spoofing Attack Capability

Number of spoofed points:

The maximum number of spoofed points could be increased if the attacker uses more advanced attack equipment. we find that **around 60 points** can be reliably spoofed in our experiments

5. Input perturbation analysis

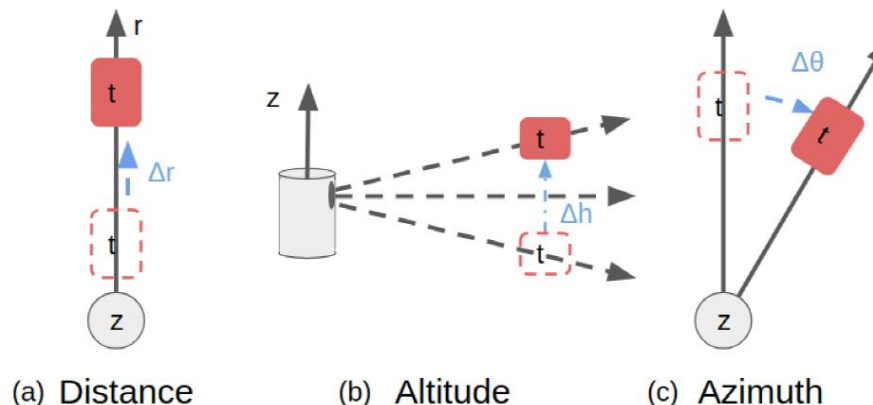
5.1 Spoofing Attack Capability

Modify the Location of spoofed points:

Distance: change the **delay of the attack laser signal pulses in small intervals** -- moving spoofed points **nearer or further** on the axis

Altitude: change the **delay in intervals of $2.304\ \mu\text{s}$** -- moving the position of the spoofed points from vertical line to vertical line to **change the height**

Azimuth: change the **delay in intervals of $55.296\ \mu\text{s}$** -- rotating the spoofed points with the LiDAR sensor as the pivot point on the **horizontal plane**



5. Input perturbation analysis

5.2 Input Perturbation Modeling

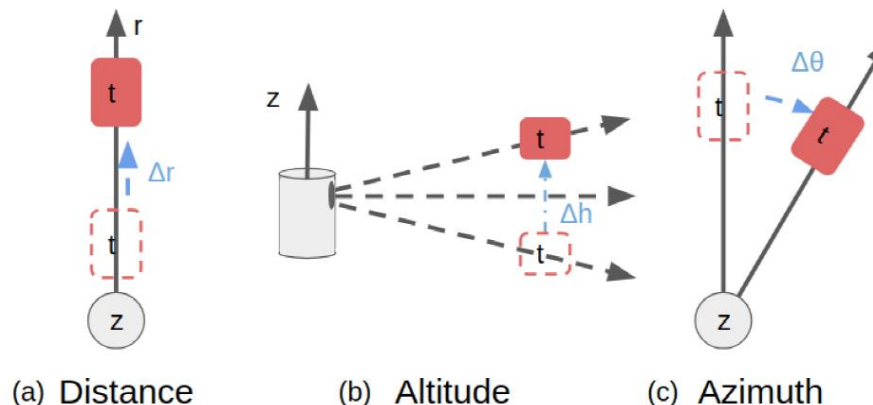
$$\begin{aligned} \min \quad & \mathcal{L}_{\text{adv}}(x \oplus t'; M) \\ \text{s.t.} \quad & t' \in \{\Phi(T') | T' \in \mathcal{A}\} \ \& \ x = \Phi(X) \end{aligned}$$

➤ Formulating merging function (\oplus)

distance: change the **delay of the attack laser signal pulses in small intervals** -- moving spoofed points **nearer or further** on the axis

Altitude: change the **delay in intervals of 2.304 μs** -- moving the position of the spoofed points from vertical line to vertical line to **change the height**

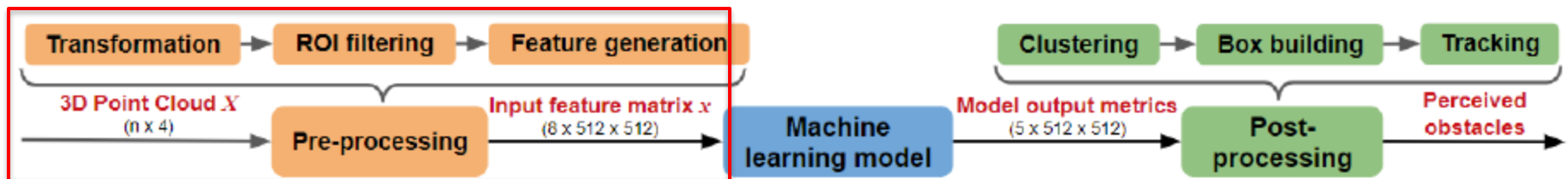
Azimuth: change the **delay in intervals of 55.296 μs** -- rotating the spoofed points with the LiDAR sensor as the pivot point on the **horizontal plane**



5. Input perturbation analysis

5.2 Input Perturbation Modeling

$$\begin{aligned} \min \quad & \mathcal{L}_{\text{adv}}(x \oplus t'; M) \\ \text{s.t.} \quad & t' \in \{\Phi(T') | T' \in \mathcal{A}\} \ \& \ x = \Phi(X) \end{aligned}$$



➤ Formulating merging function (\oplus)

1. the adversarial spoofed 3D point cloud T' will be transformed along with the 3D point cloud X . - **coordinate transformation process** has no effect
2. ROI filtering process filters out 3D point cloud located outside of the road from a bird's-eye view - as long as spoof points T' on the road, the **ROI filtering process** makes no effect
3. The feature extraction process, extracts statistical features such as average height and average intensity.

5. Input perturbation analysis

5.2 Input Perturbation Modeling

$$\begin{aligned} \min \quad & \mathcal{L}_{\text{adv}}(x \oplus t'; M) \\ \text{s.t.} \quad & t' \in \{\Phi(T') | T' \in \mathcal{A}\} \ \& \ x = \Phi(X) \end{aligned}$$

- Formulating merging function (\oplus)

$$x' = x \oplus t'$$

$$= \begin{bmatrix} \frac{I_{cnt}^x + I_{cnt}^{t'}}{(I_{avg_h}^x \cdot I_{cnt}^x + I_{avg_h}^{t'} \cdot I_{cnt}^{t'}) / (I_{cnt}^x + I_{cnt}^{t'})} \\ \max(I_{max_h}^x, I_{max_h}^{t'}) \\ \frac{(I_{avg_int}^x \cdot I_{cnt}^x + I_{avg_int}^{t'} \cdot I_{cnt}^{t'}) / (I_{cnt}^x + I_{cnt}^{t'})}{\sum I_{max_int}^x \cdot 1\{I_{max_h}^x = \max\{I_{max_h}^x, I_{max_h}^{t'}\}\}} \end{bmatrix}$$

5. Input perturbation analysis

5.2 Input Perturbation Modeling

$$\begin{aligned} \min \quad & \mathcal{L}_{\text{adv}}(x \oplus t'; M) \\ \text{s.t.} \quad & t' \in \{\Phi(T') | T' \in \mathcal{A}\} \ \& \ x = \Phi(X) \end{aligned}$$

➤ **Modeling input feature matrix spoofing capability $\Phi(\mathbf{A})$**

it equals to representing adversarial input feature matrix t' with known spoofed input feature matrix t .

We can use **global spatial transformations** including rotation, translation and scaling, under certain constraints to represent the input feature matrix spoofing capability.

5. Input perturbation analysis

5.2 Input Perturbation Modeling

$$\begin{aligned} \min \quad & \mathcal{L}_{\text{adv}}(x \oplus t'; M) \\ \text{s.t.} \quad & t' \in \{\Phi(T') | T' \in \mathcal{A}\} \ \& \ x = \Phi(X) \end{aligned}$$

➤ Modeling input feature matrix spoofing capability $\Phi(\mathbf{A})$

The location of $t_{(i)}$ can be derived as $t'_{(i)}$ as follows:

$$(u_{(i)}, v_{(i)}, 1)^T = H \cdot (u'_{(i)}, v'_{(i)}, 1)^T,$$

w.r.t. $H = \begin{bmatrix} \epsilon(\cos \theta & -\sin \theta & \tau_x \\ \epsilon(\sin \theta & \cos \theta & \tau_y \\ 0 & 0 & 1 \end{bmatrix}$

$\mathbf{t}'_{(i)}$: denote values of the i-th position on the spoofed input feature matrix \mathbf{t}'

$(\mathbf{u}'_{(i)}, \mathbf{v}'_{(i)})$: denote its location

H is a homography matrix $H(\theta, \tau, \epsilon)$

5. Input perturbation analysis

5.2 Input Perturbation Modeling

$$\begin{aligned} \min \quad & \mathcal{L}_{\text{adv}}(x \oplus t'; M) \\ \text{s.t.} \quad & t' \in \{\Phi(T') | T' \in \mathcal{A}\} \ \& \ x = \Phi(X) \end{aligned}$$

- Modeling input feature matrix spoofing capability $\Phi(\mathbf{A})$

$$t'_{(i)} = \sum_{q \in \mathcal{N}(u_{(i)}, v_{(i)})} t_{(q)} (1 - |u_{(i)} - u_{(q)}|) (1 - |v_{(i)} - v_{(q)}|),$$

$\mathbf{N}(u_{(i)}, v_{(i)})$ represents the 4-pixel neighbors (t left, top-right, bottom-left, bottom-right) at the location $(u(i), v(i))$

6. Generate adversarial examples

6.1 Design the adversarial loss

In the clustering process, each cell of the model output is filtered by its **objectness** value. After the clustering process, candidate object clusters are filtered by their **positiveness** values. Therefore, the loss function is:

$$\mathcal{L}_{adv} = \sum (1 - Q(x', \text{positiveness})Q(x', \text{objectness}))\mathcal{M}(px, py)$$

$Q(x', \cdot)$: extract the probabilities of \cdot attribute from model M by feeding in adversarial example x' .

\mathbf{M} : standard Gaussian mask

(px, py) : attack target position chosen by the attacker.

6. Generate adversarial examples

6.2 Optimization algorithm

With the Ladv design above, the optimization problem can be directly solved by using the **Adam optimizer** to obtain the transformation parameters θ , τ_x and scalar s_h by minimizing the following objective function:

$$f = \arg \min_{\theta, \tau_x, s_h} \sum (1 - Q(x', \text{positiveness})Q(x', \text{objectness}))\mathcal{M}(px, py)$$

$Q(x', \cdot)$: extract the probabilities of \cdot attribute from model M by feeding in adversarial example x' .

M : standard Gaussian mask

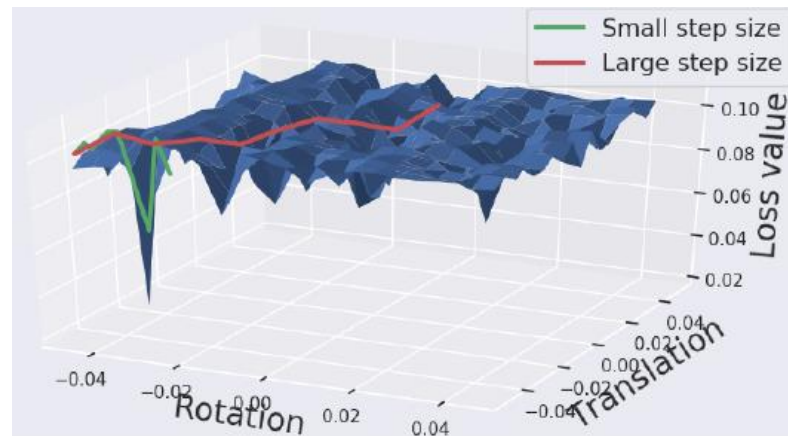
(px,py) : attack target position chosen by the attacker.

6. Generate adversarial examples

6.2 Optimization algorithm

Loss surface against the transformation parameters is as below.

Problem: loss surface over the transformation parameters is noisy at a small scale (green line) and quite flat at a large scale (red line)



Solution: 1. calculate the range of the transformation parameters so that the transformed spoofed 3D point cloud is located in the target area.
2. uniformly take n samples for rotation and translation parameters and create n^2 samples to initiate with.

6. Generate adversarial examples

6.3 Generating adversarial spoofed 3D point cloud

Using the transformation parameters θ , τ , ϵ , sh , we can express the corresponding adversarial spoofed 3D point cloud T' such that $t' = \Phi(T')$ with a dual transformation function GT of Gt .

We use T_{wx} , T_{wy} , T_{wz} to denote value of coordinate (wx, wy, wz) and T_i to denote the **value of intensity** for all points in spoofed 3D point cloud T .

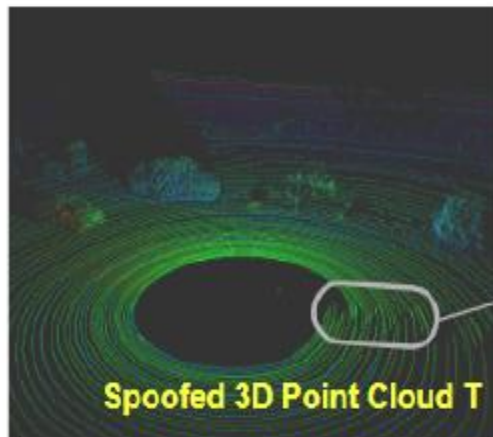
With transformation parameters θ , τ , ϵ , sh , we can express T'_{wx} , T'_{wy} , T'_{wz} of the transformed adversarial spoofed 3D point cloud T' below:

$$T'_i = T_i$$
$$\begin{bmatrix} T'_{wx} \\ T'_{wy} \\ T'_{wz} \\ 1 \end{bmatrix} = \begin{bmatrix} \cos \theta & -\sin \theta & 0 & \tau_x \\ \sin \theta & \cos \theta & 0 & 0 \\ 0 & 0 & sh & 0 \\ 0 & 0 & 0 & 1 \end{bmatrix} \cdot \begin{bmatrix} T_{wx} \\ T_{wy} \\ T_{wz} \\ 1 \end{bmatrix}$$

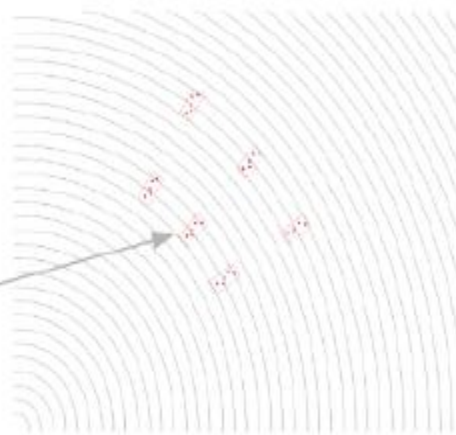
6. Generate adversarial examples

6.4 Overall adversarial example generation process

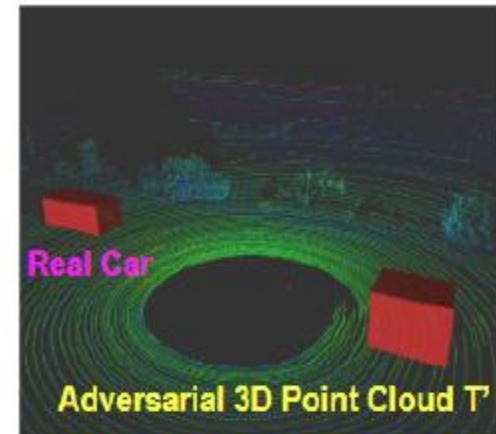
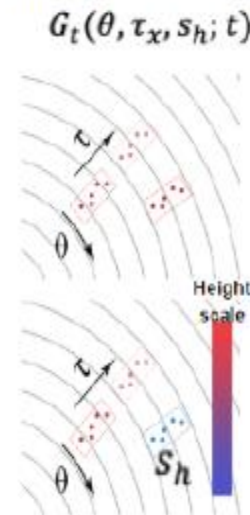
3D Point Cloud X +
Spoofed 3D Point Cloud T



Global sampling with
Spoofed Input Feature Matrix t



Global Spatial Transformation Adversarial 3D Point Cloud X'
with Spoofed Obstacle



5. Evaluation and result

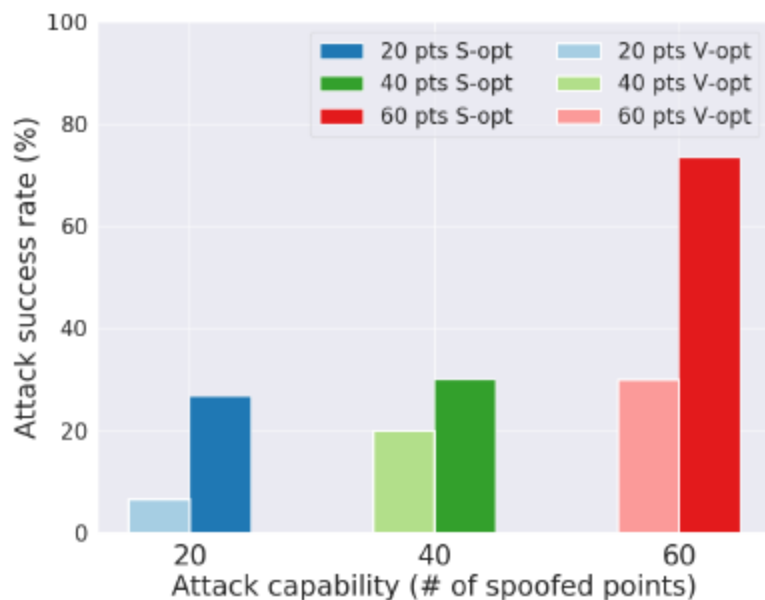


Figure 10: Attack success rate of spoofing a front-near obstacle with different number of spoofed points. V-opt refers to vanilla optimization which is directly using the optimizer and S-opt refers to sampling based optimization. We choose Adam [35] as the optimizer in both cases.

Targeted position	# Spoofed points		
	20	40	60
2-8 meters	87%	82%	90%

Table 4: Robustness analysis results of generated adversarial spoofed 3D point cloud to variation in spoofed 3D point cloud $T \in \mathcal{S}_T$. The robustness is measured by average attack success rates.

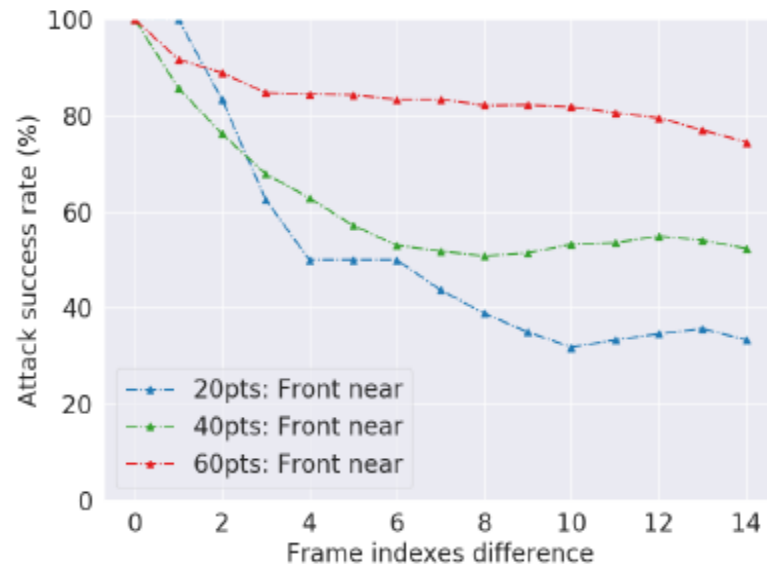


Figure 11: The robustness of the generated adversarial spoofed 3D point cloud to variations in 3D point cloud X . We quantify the variation in 3D point cloud X as the frame indexes difference between the evaluated 3D point cloud and the 3D point cloud used for generating the adversarial spoofed 3D point cloud.

Thank you
